Fusion Engineering and Design 212 (2025) 114840

Contents lists available at ScienceDirect

Fusion Engineering and Design

journal homepage: www.elsevier.com/locate/fusengdes

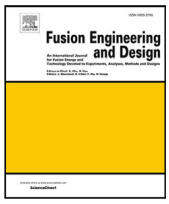

An automatic matching system for the ICRF antenna at TOMAS: Development and experimental proof

A. Adriaens [a,b,*], F. Durodié [a], V. Maquet [a], S. Deshpande [a], D. López-Rodríguez [a,b], M. Verstraeten [a], A. Goriaev [a], K. Crombé [a,b], J. Buermans [a,b], S. Brezinsek [c]

[a] Laboratory for Plasma Physics LPP-ERM/KMS, Brussels, Belgium
[b] Department of applied physics, Ghent University, Belgium
[c] Institute for Energy and Climate Research, Forschungszentrum Jülich GmbH, Germany

ARTICLE INFO

Keywords:
Antenna matching
Ion Cyclotron
Wall conditioning
Plasma Heating

ABSTRACT

The TOMAS device is equipped with an Ion Cyclotron Range-of-Frequency (ICRF) system enabling systematic investigations of Ion Cyclotron Wall Conditioning (ICWC) in a toroidal geometry complementing plasma-wall interaction and plasma production research in larger devices.

The ICRF system on the TOMAS device has a varying load as the plasma may change in density, pressure, magnetic field and species (H/D/He/Ar) depending on the required experimental conditions. Therefore, a T-matching capacitor network is installed. To correctly control these variable capacitors in order to achieve efficient power transmission to the plasma, in this paper, multiple algorithms were developed. The first kind of algorithm requires voltage probes along a coaxial line connecting the power source to the antenna, for these kinds algorithms at least 4 inputs are necessary: at least 3 voltage probe measurements along the line and the amplitude of the forward voltage, either measured directly or inferred using the requested power gain. For the second form of algorithm the amplitude of both the forward and reflected wave need to be measured as well as their phase difference. System parameters were investigated over the course of simulations and afterwards tests of one of the algorithms were carried out on the TOMAS machine, confirming its effectiveness.

1. Introduction

The TOMAS (TOroidal Magnetized System) device is located at Forschungszentrum Jülich, Germany [2]. The device has various wall conditioning systems, one of which is an Ion Cyclotron Range-of-Frequency (ICRF) antenna capable of Ion Cyclotron Wall Conditioning (ICWC). The ICRF antenna at TOMAS is a monopole [3] in a mode conversion scenario [4] which improves discharge homogeneity and wall coverage [5], and is used for material exposures in the device. As the TOMAS device is used with varying types of plasmas, a matching algorithm needed to be developed and implemented for the ICRF antenna.

An ICRF antenna system, as most antenna systems, consist of a power source, a feeding line, a matching system and an antenna. The matching system minimizes the reflection loss [6] by matching the input impedance of the load (the matching system + antenna) to the impedance of the transmission line. In most non-fusion application antenna systems the load does not change as the antenna interfaces with air or vacuum and as such a matching is chosen in the design phase after a careful calculation and/or after measurements using a VNA (Vector Network Analyser). However, as an ICRF antenna system for fusion applications has a varying load (as the plasma may vary) a controllable matching system needs to be constructed with a certain algorithm driving it.

Multiple kinds of matching systems exist in the ICRF field [7], but the algorithms developed in Section 3 should be applicable to most of them due to the inherent nature of matching systems, the algorithm used on TEXTOR [8] directly follows and the one used on JET [9] indirectly follows (as it is higher in dimensionality).[1]

As will be explained in Section 2, the ICRF antenna at TOMAS has computer-controlled variable capacitors as a matching circuit, similar to the ones used in TEXTOR, the matching algorithms were simulated on the TOMAS circuit as shown in Section 4 one of the algorithms was then tested on the TOMAS device, as explained in Section 5.2.

* Corresponding author at: Department of applied physics, Ghent University, Belgium.
E-mail address: arthur.adriaens@mil.be (A. Adriaens).

[1] Note that the ICRF system at W7-X, at the time of writing, is not able to use a continuous feedback algorithm due to the possibility of arcs, the algorithm used there thus differs [1].

https://doi.org/10.1016/j.fusengdes.2025.114840
Received 4 October 2024; Received in revised form 27 January 2025; Accepted 28 January 2025
Available online 8 February 2025

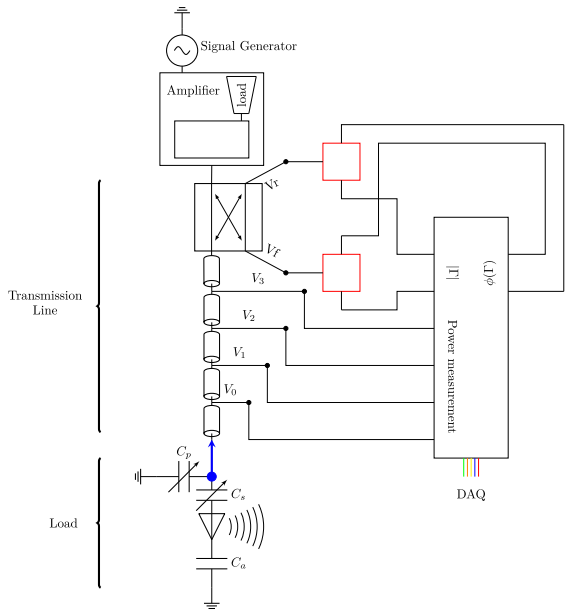

Fig. 1. The top left AC power source symbolizes a signal generator which may generate a signal in the range of 10 MHz–50 MHz connected to an amplifier which may amplify the signal up to 6 kW of power. To measure valuable information needed for the algorithms that will be introduced, there is a power and phase measurement box (rightmost square) to which various probes are connected. Such as the voltage probes V_0-V_3 in the line connecting the amplifier to the antenna system and probes V_f and V_r which may measure, using the directional coupler (symbolized as a box with arrows), the forward power (the power going down to the antenna) and the reflected power (the power which was not injected into the plasma and goes back up to the amplifier). The square red boxes are splitters so that both the forward and reflected power and their difference in phase may be measured at the directional coupler. (Γ indicates the ratio of the reflected over forward power.)

2. Overview of the ICRF antenna circuit

The antenna circuit used in TOMAS is shown in Fig. 1, the power may be imagined to flow from top to bottom, going from the amplifier output through a directional coupler, making it possible to measure the forward and reflected voltages, after which it goes through a coaxial line with embedded voltage meters. The signal then gets to a T capacitor matching section (I.e the C_p and C_s variable capacitors). After this it goes to the antenna, of which a CAD model is shown in Fig. 2, here the power is split in two, half goes downwards and gets reflected at the vessel and the other half goes upwards into the pre-matching capacitor C_a where it also gets reflected, this one needs to be chosen in such a way (dependent on the frequency) that the vessel reflected current and the pre-matching capacitor reflected current cancel out (due to being in opposite phase) reducing the voltage on the antenna. Whilst these oscillating currents move along the antenna strap, power gets radiated into the plasma. If the system is not perfectly "matched", meaning that not all the power may enter the load, then a part may return back up the chain to the amplifier which handles this by dumping the power in a dummy load. The characteristics of the capacitors used to match the antenna to the plasma are listed in Table 1. During the simulations, discretization of 16 000 possible positions for the pre-matching capacitor and 10 000 each for C_s and C_p will be used in accordance with the actual possible capacitor positions, as they are limited by the minimum step size of the stepper motor.

3. Derivation of the algorithms

3.1. Inferring the load reflection coefficient

Looking from the end of the transmission line towards the amplifier, the chosen 0 position shown as a blue dot and the positive direction

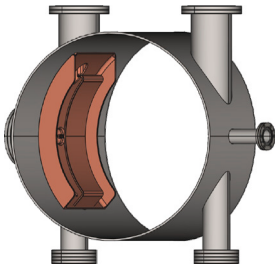

Fig. 2. The antenna strap in the vessel, the leftmost port connects to the series and parallel capacitors whilst the top port of the strap connects to the pre-matching capacitor.

Table 1
The listed capacitors are driven by a stepper motor with a step size of 0.9°, as such the pre-matching capacitor (C_a) has ≈16 000 possible positions and the others (C_s and C_p) have ≈10 000.

Name	Model	V_{max} (kV)	I_{max} (A)	C-range (pF)	Turns
C_a	Comet CV2C 1000	40	138	35–1000	≈40
C_s	CVDD-1000-10S	6	140	25–1000	≈25
C_p	Jennings CVCH-1000-5	5	70	7–1000	≈25

as a blue arrow in Fig. 1, from transmission line theory, a forward and reflected voltage wave along the line of the following form are expected (time harmonic convention iωt):

$$V_f(l) = |V_f|e^{i\Phi_f(l)} = |V_f|e^{-i\beta l}e^{i\phi_f} \tag{1}$$

$$V_r(l) = |V_r|e^{i\Phi_r(l)} = |V_r|e^{i\beta l}e^{i\phi_r} \tag{2}$$

With l the distance from the load, β the wavenumber of the signal and $\phi_{f/r}$ a phase. The total voltage along the transmission line is given by:

$$\begin{aligned} V(l) &= V_f(l) + V_r(l) \\ &= |V_f|e^{i\phi_f}\left(e^{-i\beta l} + \frac{|V_r|}{|V_f|}e^{i(\phi_r-\phi_f)}e^{i\beta l}\right) \\ &:= |V_f|e^{i\phi_f}\left(e^{-i\beta l} + \Gamma_L e^{i\beta l}\right) \\ &:= V^+\left(e^{-i\beta l} + \Gamma_L e^{i\beta l}\right) \end{aligned}$$

where the *reflection coefficient at the load* Γ_L was defined, the voltage at probe i is given by:

$$V_i = V^+(e^{-i\beta l_i} + \Gamma_L e^{i\beta l_i}) \tag{3}$$

with l_i the distance from the load to probe i. Defining $\Gamma_L := u + iv$, it can be derived that

$$\frac{|V_i|^2}{|V^+|^2} = 1 + u^2 + v^2 + 2u\cos(2\beta l_i) - 2v\sin(2\beta l_i) \tag{4}$$

Using the voltage measurements at the points along the line $|V_{0-3}|$ and the measured (at the directional coupler) forward voltage amplitude $|V^+|$, a system of 4 linear equations can be constructed and solved. Defining

$$\mathbb{C}_i := \cos(2\beta l_i) \quad \mathbb{S}_i := \sin(2\beta l_i) \tag{5}$$

And

$$\frac{|V_i|^2}{|V^+|^2} - 1 =: \mathcal{V}_i \tag{6}$$

Either this set of equations is solved for u and v using all 4 voltage probes:

$$u = \frac{1}{2}\frac{(\mathcal{V}_0 - \mathcal{V}_1) - (\mathcal{V}_2 - \mathcal{V}_3)\left(\frac{\mathbb{S}_0-\mathbb{S}_1}{\mathbb{S}_2-\mathbb{S}_3}\right)}{(\mathbb{C}_2 - \mathbb{C}_3)\left[\left(\frac{\mathbb{C}_0-\mathbb{C}_1}{\mathbb{C}_2-\mathbb{C}_3}\right) - \left(\frac{\mathbb{S}_0-\mathbb{S}_1}{\mathbb{S}_2-\mathbb{S}_3}\right)\right]} \tag{7}$$

$$v = \frac{1}{2}\frac{(\mathcal{V}_0 - \mathcal{V}_1) - (\mathcal{V}_2 - \mathcal{V}_3)\left(\frac{\mathbb{C}_0-\mathbb{C}_1}{\mathbb{C}_2-\mathbb{C}_3}\right)}{(\mathbb{S}_2 - \mathbb{S}_3)\left[\left(\frac{\mathbb{C}_0-\mathbb{C}_1}{\mathbb{C}_2-\mathbb{C}_3}\right) - \left(\frac{\mathbb{S}_0-\mathbb{S}_1}{\mathbb{S}_2-\mathbb{S}_3}\right)\right]} \tag{8}$$

Using only 3 of the 4 voltage probes denominated as a, b and c:

$$u = \frac{1}{2}\frac{(\mathcal{V}_a - \mathcal{V}_b) - (\mathcal{V}_b - \mathcal{V}_c)\left(\frac{\mathbb{S}_a - \mathbb{S}_b}{\mathbb{S}_b - \mathbb{S}_c}\right)}{(\mathbb{C}_b - \mathbb{C}_c)\left[\left(\frac{\mathbb{C}_a - \mathbb{C}_b}{\mathbb{C}_b - \mathbb{C}_c}\right) - \left(\frac{\mathbb{S}_a - \mathbb{S}_b}{\mathbb{S}_b - \mathbb{S}_c}\right)\right]} \tag{9}$$

$$v = \frac{1}{2}\frac{(\mathcal{V}_a - \mathcal{V}_b) - (\mathcal{V}_b - \mathcal{V}_c)\left(\frac{\mathbb{C}_a - \mathbb{C}_b}{\mathbb{C}_b - \mathbb{C}_c}\right)}{(\mathbb{S}_b - \mathbb{S}_c)\left[\left(\frac{\mathbb{C}_a - \mathbb{C}_b}{\mathbb{C}_b - \mathbb{C}_c}\right) - \left(\frac{\mathbb{S}_a - \mathbb{S}_b}{\mathbb{S}_b - \mathbb{S}_c}\right)\right]} \tag{10}$$

Or, as was the case for the systems used in TEXTOR [8] due to the want to use high speed analogue electronic feedback circuits, Taylor expand Eq. (4) to first order in u and v and solve using 2 voltage probes denominated as a and b:

$$u = \frac{1}{2}\frac{\mathcal{V}_a(1-\mathbb{S}_b) - \mathcal{V}_b(1-\mathbb{S}_a)}{(1+\mathbb{C}_a)(1-\mathbb{S}_b) - (1+\mathbb{C}_b)(1-\mathbb{S}_a)} \tag{11}$$

$$v = -\frac{1}{2}\frac{\mathcal{V}_a(1-\mathbb{C}_b) - \mathcal{V}_b(1-\mathbb{C}_a)}{(1+\mathbb{C}_a)(1-\mathbb{S}_b) - (1+\mathbb{C}_b)(1-\mathbb{S}_a)} \tag{12}$$

There is also another way of finding out u and v, as both the amplitude of Γ and its phase at the directional coupler are measured, it is possible to reconstruct Γ_L, this may be done by shifting it from the coupler position to the load position:

$$\Gamma = \rho e^{i\phi} \rightarrow \Gamma_L = \rho e^{i(\phi - 2\beta l_{dir})} \tag{13}$$

With l_{dir} the distance between the load and the directional coupler.

3.2. Constructing error variables

Now that $\Gamma_L = u + iv$ is known it may be transformed to find that the admittance is given by

$$Y_L = \frac{1-\Gamma_L}{1+\Gamma_L} = \frac{1-u^2-v^2}{(1+u)^2+v^2} - i\frac{2v}{(1+u)^2+v^2} \tag{14}$$

Perfect RF matching (I.e no reflection) occurs when $\Re\{Y_L\} := g = 1$ and $\Im\{Y_L\} := b = 0$. So, to probe the distance to matching, the following error variables are introduced:

$$\epsilon_g \propto 1 - \frac{1-u^2-v^2}{(1+u)^2+v^2} \quad \text{and} \quad \epsilon_b \propto \frac{2v}{(1+u)^2+v^2} \tag{15}$$

or

$$\epsilon_g := u^2 + v^2 + u \qquad \text{and} \qquad \epsilon_b := v \tag{16}$$

Using transmission line theory (Eq. (3)) the TOMAS coaxial line was simulated with a starting Γ_L. After inferring the simulated voltage at the locations where the various real probes would be, u and v were computed using the methods discussed in the previous subsection making it possible to obtain the error variables for the different amount of probes using Eqs. (16). Afterwards the system was changed according to

$$Y_{\text{corrected}} = Y_{\text{initial}} + \epsilon_g + i\epsilon_b \tag{17}$$

Fig. 3 shows the difference between the initial and final Γ_L (by transforming the corrected admittance back to a reflection coefficient) for different starting configurations. It can be concluded that changes in the direction of the error using all 4 voltage probes, 3 voltage probes or the directional coupler, will theoretically always correct the reflection coefficient in a relatively straightforward path which is in contrast to the linearized approach using 2 voltage probes which was done at TEXTOR which, although able to match the system close to $\Gamma = 0$, does so in a non-direct way.

3.3. Change the capacitances accordingly

As the parallel capacitor can only influence the imaginary part of the admittance, to match the system, the change in capacitances will approximately have to vary as:

$$\delta C_s \propto -\epsilon_g \quad \text{and} \quad \delta C_p \propto -\epsilon_b \tag{18}$$

This same kind of proportionality is also used in TEXTOR and JET [9] as it is a general property of matching systems, as long as you have 2 components to separately influence the real and imaginary parts of the admittance, you can construct error variables and set them proportional. As both variable capacitors on TOMAS are linear, the amount of steps (or in the simulation, change in capacitance) required may be given by

$$\Delta C_s = -S(\Gamma, \ldots)\epsilon_g(\phi) \tag{19}$$

$$\Delta C_p = -P(\Gamma, \ldots)\epsilon_b(\phi) \tag{20}$$

With S and P functions which we may let depend on a number of variables, free to our choosing to influence the behaviour of the algorithm (e.g big steps/fast when high reflection and slow when precise adjustments need to be made) both will be set to 1 pF in the simulation for now as the TOMAS matching device has identical capacitors used for both the real and imaginary parts, if different systems are mixed (e.g a line stretcher and a phase shifter or 2 non-equal capacitors) these functions are not necessarily equal. The optimal size and Γ dependence of these functions may be inquired through simulation.

3.4. Algorithms

The previous sections can be summarized in four main possible algorithms. The procedures for the various algorithms are quite straightforward, the first step is to measure the forward voltage. After this u and v need to be determined. As explained previously, the possible ways are:

- *3 V algorithm:* measuring the voltage at 3 probe positions a,b and c and using Eqs. (9) and (10) to infer u and v
- *4 V algorithm*: measuring on 4 probes and using Eqs. (7) and (8) to infer u and v
- *Directional Coupler algorithm:* measuring the reflected voltage and the phase difference between V_r and V_f fully infers the complex-valued Γ at the directional coupler. This value then needs to be phase shifted to the load with Eq. (13), yielding u and v.
- *TEXTOR* algorithm: using 2 probes and Eqs. (11) and (12) to infer u and v.

Then the steps for all the algorithms are the same: using Eq. (16) to get the errors, and move the capacitors according to Eqs. (19) and (20).

4. System analysis

The full circuit was simulated using the open source software pyRFtk [10], enabling us to test its behaviour under the matching algorithms. The circuit model is made up of the scattering (S) matrices of all the components involved (transmission line, capacitors, ...) most of the required components have ideal counterparts modelled in pyRFtk, the only thing missing was the antenna in a plasma, this was simulated using HFSS [11,12] making use of a low-density ($n_e = 5{\times}10^{16}$ m^{-3}) homogeneous hydrogen cold plasma dielectric [13] in a simplified TOMAS geometry with periodic boundary conditions[2] with the antenna model from when it was designed. The simulation setup is shown in Fig. 4. Changes in plasma species and density are expected to change the frequency response but are outside the scope of this work.

4.1. Algorithm matchability comparison

Given a well-chosen C_a (how this was chosen will be explained in Section 4.3) and some initial C_s and C_p, examples of simulated system evolutions following these algorithms are shown in Fig. 5. Henceforth the RF definition that the system is *matched* if $|\Gamma| < 0.1$ will be used unless stated otherwise. The various algorithms may be quantitatively

[2] Whilst the simulation is thus as if we have an antenna array, due to the low density and antenna power, this approximation should suffice.

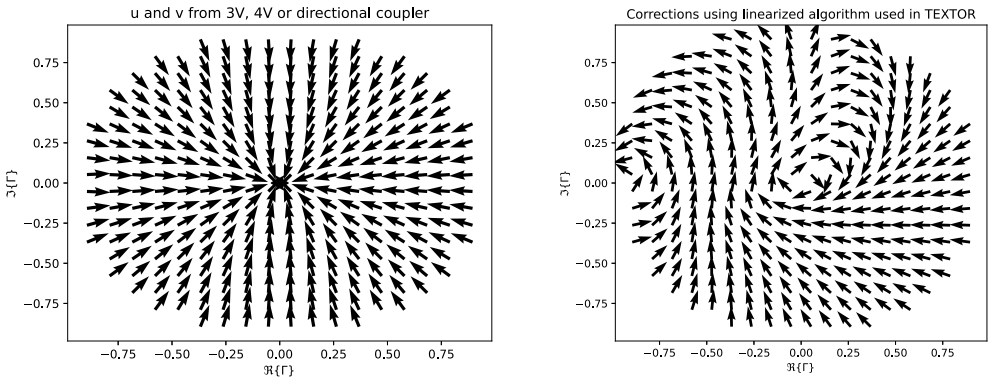

Fig. 3. The left quiver plot looks the same for u and v computed using 3 voltage probes, 4 voltage probes and with gamma from the directional coupler with added phase shift, the convergence to the wanted $\Gamma = 0 + i0$, or 0 reflection, is clear to see contrary to the linearized approach on the right. Note that the right plot does not change much if other voltage probe combinations are used.

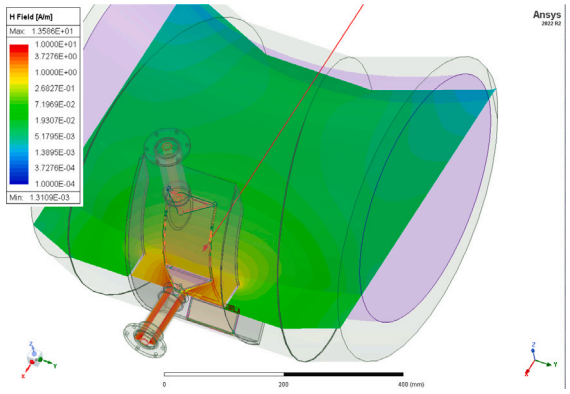

Fig. 4. A screenshot of HFSS showing a magnetic field simulation of the ICRF antenna in the reduced TOMAS geometry with periodic boundary conditions (at the left and right sides of the model).

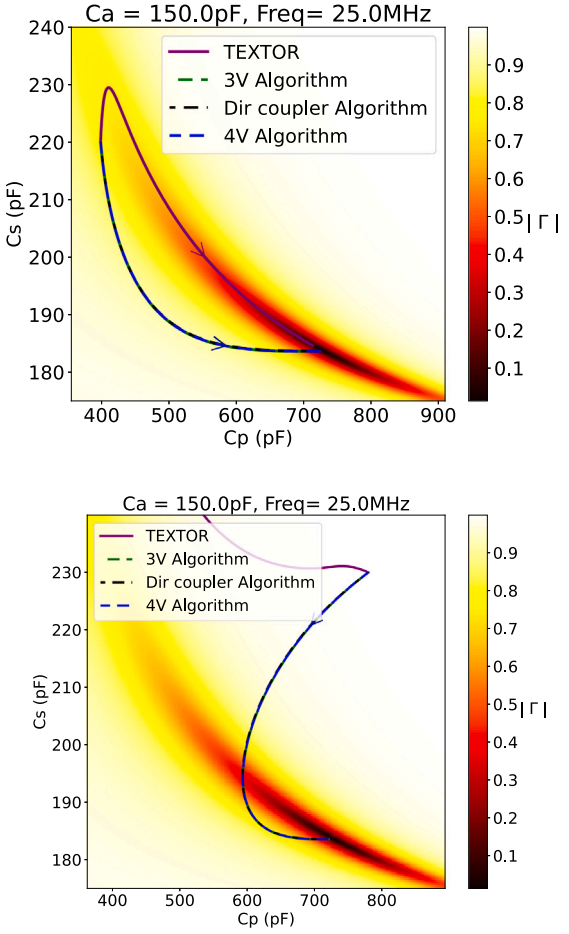

Fig. 5. For every possible C_s, C_p combination shown the reflection coefficient is computed and its norm displayed as a colour map. The system is then evolved from two randomly chosen initial C_s, C_p positions, one on the top and one on the bottom figure, according to the introduced algorithms with S = P = 1 pF until it reaches $\Gamma = 0.05$. The linearized, or "TEXTOR", algorithm fails to match the system in the bottom case.

compared by how big their matchable domain is (the matchable domain is the amount of initial C_p, C_s combinations from which the algorithm is able to match the system), an example comparison at 25 MHz for 1 kW forward IC power is given in Fig. 6. The 3 V/4 V and directional coupler all behave the same, as expected theoretically, and match the system from 84% of the initial capacitor positions, 100% was likely not achievable due to the approximation made in Eq. (18), however this was deemed sufficient for device operation. This is in contrast to the algorithm used at TEXTOR to drive the capacitors which is only able to match close to the solution (8% of the region), however, as TEXTOR's capacitor system was used as a fine correction system to perfect the matching (main matching was done using a different system), its low matchable domain was not an issue for TEXTOR operation.

4.2. Finding a good S and P

As is clear from Eqs. (19) and (20), S and P are free parameters in the algorithm. These factors will influence the step size taken in the capacitors, as will be explained in Section 5.2 the algorithm works sequentially for now with plans of making it continuous in the future, as such this will now greatly influence how fast the algorithm matches the system. The simplest form of finding both S and P will be done by setting them equal to the same constant S = P = SPFactor and varying this constant, looking at the matchable fraction (from within the green area in Fig. 6) and the amount of changes to the capacitor positions (or amount of steps). The result for the directional algorithm is shown in Fig. 7. Good S and P coefficients occur at S = P = 55 pF where the matchability is still at 100% compared to when S = P = 1 pF and the average steps needed to match the system are at a near minimum (≈50). To continue the match to even smaller reflections the constants are reverted back to S = P = 1 pF, i.e S = P = 55 pF when $\Gamma > 0.1$ and S = P = 1 pF when $\Gamma < 0.1$. If a matching simulation is carried out this way, stopping at 4%, you get Fig. 8 showcasing the effectiveness of using S = P = 55 pF in speeding up the algorithm whilst keeping the accuracy. A

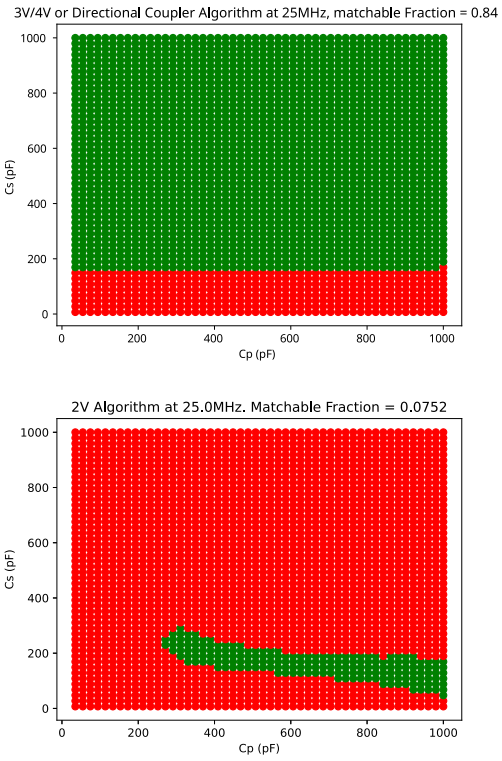

Fig. 6. The green dots indicate the initial positions from which the system may be matched whilst the red dots indicate the opposite. The *matchable fraction* is the fraction of green dots over total dots.

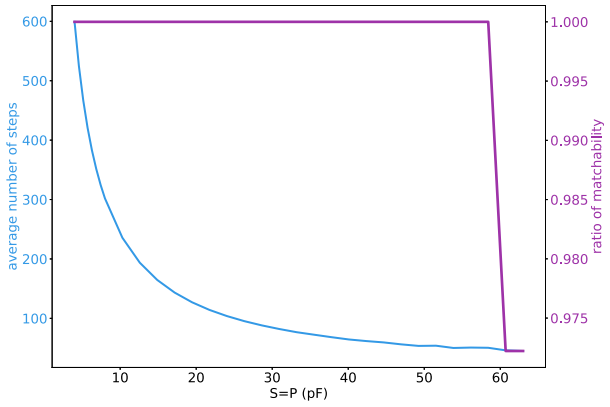

Fig. 7. Positions within the green domain shown in Fig. 6 were used as starting positions for each S = P value, the system was then evolved using the directional coupler algorithm recording the average amount of steps and the matchability (1 meaning all initial positions were matchable).

more sophisticated analysis could determine functions with dependence on Γ for S and P as mentioned in Eqs. (19) and (20), however we will work with the mentioned step system (big when $\Gamma > 0.1$ and small once $\Gamma < 0.1$).

4.3. Choosing the pre-matching capacitor value C_a

As the algorithms are only able to determine how C_s and C_p need to move, the pre-matching capacitor (C_a) will have to be chosen in advance. The ideal pre-matching capacitor value would minimize the voltage and currents at the feedthrough[3] and is almost purely dependent on the frequency (as it concerns the phase difference which is dependent on the wavelength). This value for C_a could be determined through simulation, however, it could also be found by measuring the RMS (Root Mean Square) currents at the capacitors. In the system this may be verified using the current probes installed close to the capacitors. To get some insight in how the system will behave, a pre-matching capacitor scan was simulated at a fixed frequency. The size of the *matchable domain*, the C_s and C_p combinations at which $|\Gamma| < 0.1$, and the maximal coupled current through the capacitors in the domain (which was normalized with respect to the coupled power) were monitored. The result is shown on the left in Fig. 9. A local minimum occur in the maximum RMS current ratio just before $C_a = 170$ pF, whilst the amount of matched combinations is reasonably large. In the same way, the pre-matching capacitor values can be found for other frequencies, if the same conditions are carried out throughout it is found that the pre-matching capacitance should go down exponentially with frequency, in particular, according to simulations it should follow

$$C_a(f) = ae^{-bf} + c \approx 2325e^{\frac{0.101}{\text{MHz}}f}\ \text{pF} + 31\ \text{pF} \tag{21}$$

In the range [19 MHz:50 MHz], 19 MHz being the lower limit due to C_p reaching its maximum value and 50 MHz the upper limit as the amplifier is rated 10–50 MHz. As the T-matching box on TOMAS contains a current probe, the pre-matching capacitor dependence of the currents will be verified in Section 5.2 and the validity of Eq. (21) will be verified in future studies.

5. Test of the algorithm on the TOMAS device

5.1. Measurement systems and calibration

To obtain accurate measurements, the various components were calibrated, the reader is requested to consult Fig. 1 during the explanation. First all the connectors of the directional coupler were connected to a VNA (Vector Network Analyser) and frequency scans were performed, confirming that the directional coupler attenuates the Vf and Vr output by 70 dB (which was listed on its data sheet). Then the various plugs on the line were measured, obtaining a 6 × 6 scattering matrix from which we know the attenuation on the voltage probes.[4] To calibrate the power measurement circuits (AD8307) and phase measurement circuits (AD8302), the VNA was connected to the voltage in ports (i.e the inputs of the splitters, V_r and V_f on the circuit, and the inputs of the voltage probe measurements, V_{0-3} on the circuit), whereby power ramps where performed with the corresponding voltages measured on the DAQ (Data AQuisition system). As the VNA was calibrated, these power measurements (in voltage over time) could be linked to the input power ramp (power over time) to create voltage-power relations for every specific input. To calibrate the phase measurement system a circuit was constructed consisting of a splitter, one of the outputs going to a line stretcher and the other a coaxial cable , the line stretcher was connected to V_r and the coax cable to V_f after which multiple settings of the line stretcher were used, a constant frequency (100 MHz) was supplied from the VNA and corresponding voltages measured on the DAQ, later the induced phase difference for each line stretcher setting were measured using the VNA, enabling the relation Voltage-phase shift. The only systems not calibrated are the current probes near the capacitor (similar in design to the voltage probes along the line) as there was no easy way of doing so. But as the intend is to look at the behaviour, rather than the absolute values, this did not

[3] A vacuum part which connects the T-matching circuit, outside of the vessel, to the strap, inside of the vessel.

[4] The transmission line is a coaxial line with an inner copper conductor and an outer aluminium shell, the voltage probes are set in the aluminium, floating above the copper line.

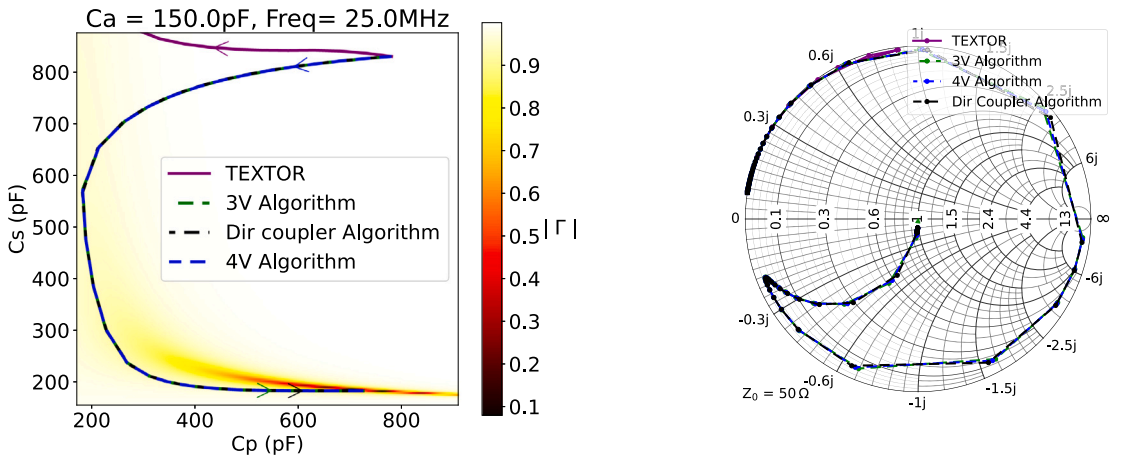

Fig. 8. From a very bad starting position, the new algorithms (note TEXTOR going outside the figure) are able to match the system to 4% reflection in about 90 steps.

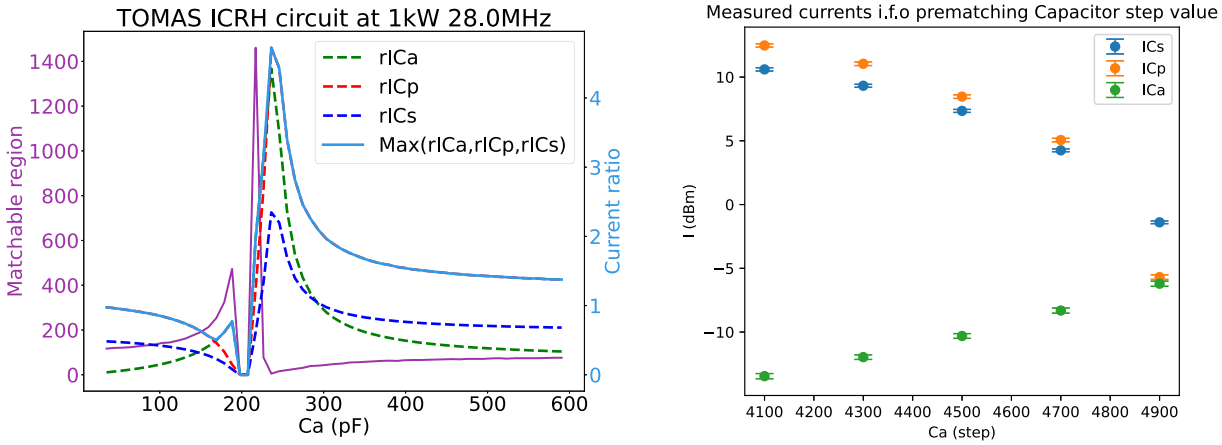

Fig. 9. The figure on the left shows the simulated pre-matching capacitor scan. The purple curve was computed by matching the circuit for the specified pre-matching capacitor value and creating a local square of 10 pF (in C_s, C_p space) around the matched position, counting how many positions had $\Gamma < 0.1$, the current curves show the current ratio (computed RMS current over the capacitor limit RMS current) at the matched position. As is seen around the 200 pF mark, theoretically a region where the system is not matchable is expected which was also observed experimentally. On the right, measurements of the current on the physical TOMAS device are shown which were carried out using non-calibrated current probes positioned close to the respective capacitors, returning an oscillating voltage which was measured as RF power in dBm.

pose an issue. During testing it seemed that the voltage probes did not provide realistic measurements (sometimes powers more than 2 times higher than the input power were measured) which may be caused by amplifier harmonics (which also was an issue on TEXTOR), noise, or an incorrect calibration. This problem was however not observed in the directional coupler.

5.2. Implementation and result

A diagram of the implementation on the TOMAS device is shown in Fig. 10, the procedure works as follows: The control PC (PC1) instructs an IC (Ion cyclotron) discharge (low power at first, higher when almost matched), either whilst simultaneously using EC (Electron cyclotron) or with a short EC discharge beforehand (as EC is able to ionize the plasma when the density is low, this is not possible for IC at TOMAS). It also triggers the DAQ (PC2) to collect data, PC2 collects the needed measurements and sends it over to PC1 via UDP, PC1 then goes through the steps explained in Section 3 to compute how the capacitors should move and instructs the arduino to move the attached stepper motors to the new position. Then it repeats the process. The procedure can be broken down in the following steps: First the data is sampled for 0.7 s of which 0.5 s are discharge (a delay of 0.2 s is observed at the DAQ), then the capacitor is moved (which, from observations, happens near instantaneous) after which a 3 s delay is held to make

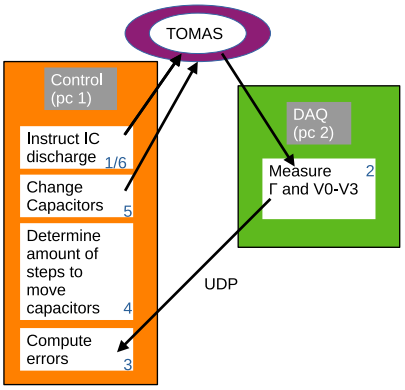

Fig. 10. As the last value of the discharge measurement are sent over via UDP (User Datagram Protocol), noise can have a huge impact.

sure the plasma may return to its original pressure and density. In total one step thus takes ≈4 s. The matching process could be made faster by continuously moving whilst doing a discharge, this will be discussed in Section 6. In Fig. 11 a demonstration of this principle,

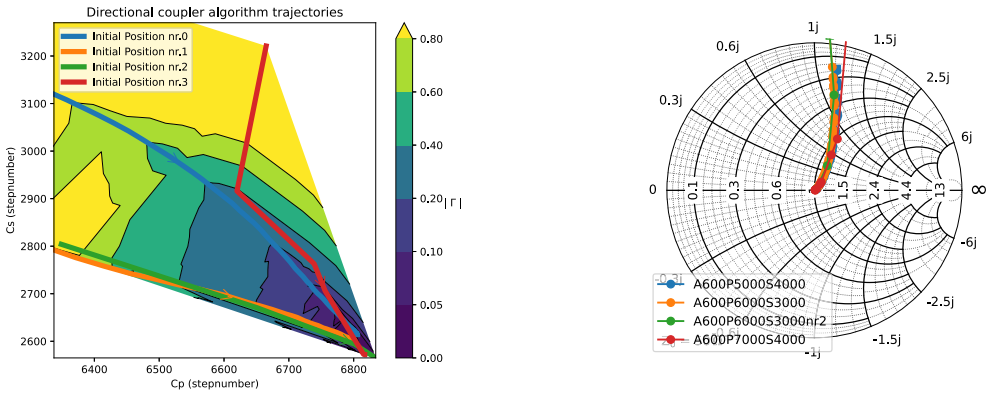

Fig. 11. Here some trajectories measured on the real system at 40 MHz using the directional coupler algorithm are shown, on the left is capacitor space (the numbers implying the amount of steps from the origin) with the colour map a tricontour interpolation of the directional-coupler measured $|\Gamma|$. Note that, as in the simulations, we assume the system is not matchable using the algorithm if C_s is sufficiently below the matched point, as such, all paths were started sufficiently high up. Note that the red trajectory had a bigger step size than the blue trajectory. Also note that position nr.0 was started at (Cp = 5000, Cs = 4000), but cut short for illustrative purposes. On the right plot is the measured full form of Gamma, phase rotated to the load position (with the labels representing the initial step positions, e.g position 0 was at prematching 600 parallel 5000 and series 4000 initially).

tested on the machine, is shown. The directional coupler algorithm evolves multiple high Γ initial positions to the "matched" region. Note that the algorithm is not able to start as far back from a matched position as in the simulations as the accuracy of the measured Γ is reduced, this might be caused by the noise picked up by the cables connecting the power measurement circuits and the DAQ (this is a reoccurring problem in TOMAS). Nevertheless, as shown, the algorithm does seem to perform quite well when the capacitors are not "too far" from the final position. For example, the blue trajectory in Fig. 11 which started at position $C_s = 5226$, $C_p = 3847$ (but of which the first 10 steps are not displayed for clarity) reached $\Gamma = 0.01 \pm 0.003$ in 64 steps, or ≈256 s. This trajectory was quite long and served more as a test of the algorithm, a more general trajectory whereby we had started closer to the previously good working conditions would be closer to ≈64 s. From testing it is clear that the directional coupler algorithm enables fairly rapid antenna matching enabling less power loss and less stress on the dummy load of the amplifier. Using this algorithm, various pre-matching capacitor positions were matched for 28 MHz, as is shown on the right panel of Fig. 9, As the probes were not calibrated, it is only possible to look at the relative behaviour, not their values. However despite this restriction, it is still possible to recognize the exponential fall of IC_s and IC_p with a rise of IC_a in the experiment, as is the case before $C_a = 170$ pF in the simulation, proving that the ideal position on the physical device should lie somewhere close to the explored region (as this behaviour on the simulated device corresponds with a stable local minimum in currents on the capacitor). Later on it should be possible to fit the experimental data to the simulation by finding the exact boundary when the system becomes unmatchable, thus finding the optimal pre-matching capacitor position for the corresponding frequency.

6. Plans for improved implementation

As mentioned previously, the plan is to set up a continuous feedback system to match the system during a discharge. This would be implemented by connecting the output voltages of the power and phase measurement box – which now go to the DAQ – to an integrated circuit which would compute the needed change to the capacitors and drive the motors directly. In theory this makes it so that one cycle, i.e measuring the voltages, processing the signals and moving the capacitors, would mostly be bottlenecked by the speed of the motors. The motors are set to have a delay of 1 ms between pulses, with 4 pulses per step, achieving very high accuracy but relatively low speed. A very bad match as the one shown in Fig. 8 needs to change the parallel capacitor with around 600 pF (as it moves back an forth) and the series with around 600 pF to match the system, as the capacitors move with about 0.05 pF per pulse this means at most 12 000 pulses (as they are able to move in parallel) or 12 s for a really bad initial position. Note that most starting positions will be under 200 pF away from the matched position, taking less than 4 s.

7. Conclusion

General matching algorithms were derived and implemented on the TOMAS device. After testing it became clear that the directional coupler algorithm had superior performance and was thus chosen over algorithms relying on voltage probes. All matching systems derived over the course of this work leverage the same principle: finding the reflection coefficient at the load Γ_L makes it possible to construct error variables, which are linearly related to the needed changes in the matching system. However, the algorithms arrive at the same answer in different ways, either the voltages along the line are measured or the forward, reflected voltage and their phase difference at the directional coupler are measured. As the concept is fairly general it should be deployable on other devices and in other fields as long as Γ_L may be determined and the real and imaginary part of the admittance are independently receptive to matching component changes.

8. Addendum

8.1. Defence statement

This work is funded by Belgian defence under project DFR-MSP23-07.

8.2. Eurofusion statement

This work has been carried out within the framework of the EUROfusion Consortium, funded by the European Union via the Euratom Research and Training Programme (Grant Agreement No 101052200 — EUROfusion). Views and opinions expressed are, however, those of the authors only and do not necessarily reflect those of the European Union or the European Commission. Neither the European Union nor the European Commission can be held responsible for them.

CRediT authorship contribution statement

A. Adriaens: Writing – review & editing, Writing – original draft, Visualization, Validation, Software, Methodology, Investigation, Formal analysis, Data curation, Conceptualization. **F. Durodié:** Software, Formal analysis. **V. Maquet:** Software, Investigation, Formal analysis. **S. Deshpande:** Writing – review & editing, Validation, Software, Investigation. **D. López-Rodríguez:** Writing – review & editing, Data curation. **M. Verstraeten:** Conceptualization. **A. Goriaev:** Writing – review & editing, Supervision, Project administration, Data curation, Conceptualization. **K. Crombé:** Writing – review & editing, Supervision. **J. Buermans:** Writing – review & editing. **S. Brezinsek:** Resources.

Declaration of competing interest

The authors declare that they have no known competing financial interests or personal relationships that could have appeared to influence the work reported in this paper.

Data availability

Data and codes are publicly available on github, a hyperref link is embedded in the paper.

References

[1] I. Stepanov, J.P. Kallmeyer, D.A. Hartmann, M. Vervier, D. Castaño-Bardawil, P. Dumortier, F. Durodié, H. Faugel, K.P. Hollfeld, M. Verstraeten, G. Offermanns, J. Ongena, G. Satheeswaran, B. Schweer, M. Van Schoor, K. Crombé, Ye. O. Kazakov, S. Acheroy, M. Vergote, R. Wolf, Setup and first operation of the wendelstein 7-X ICRH matching system, Fusion Eng. Des. (ISSN: 0920-3796) 211 (2025) 114794, http://dx.doi.org/10.1016/j.fusengdes.2024.114794, URL https://www.sciencedirect.com/science/article/pii/S0920379624006446.

[2] A. Goriaev, T. Wauters, S. Möller, R. Brakel, S. Brezinsek, J. Buermans, K. Crombé, A. Dinklage, R. Habrichs, D. Höschen, M. Krause, Yu. Kovtun, D. López-Rodríguez, F. Louche, S. Moon, D. Nicolai, J. Thomas, R. Ragona, M. Rubel, T. Rüttgers, P. Petersson, P. Brunsell, Ch. Linsmeier, M. Van Schoor, The upgraded TOMAS device: A toroidal plasma facility for wall conditioning, plasma production, and plasma–surface interaction studies, Rev. Sci. Instrum. (ISSN: 0034-6748) 92 (2) (2021) 023506, http://dx.doi.org/10.1063/5.0033229, arXiv:https://pubs.aip.org/aip/rsi/article-pdf/doi/10.1063/5.0033229/10050393/023506_1_online.pdf.

[3] F. Louche, T. Wauters, R. Ragona, S. Möller, F. Durodié, A. Litnovsky, A. Lyssoivan, A. Messiaen, J. Ongena, P. Petersson, M. Rubel, S. Brezinsek, Ch. Linsmeier, M. Van Schoor, Design of an ICRF system for plasma–wall interactions and RF plasma production studies on TOMAS, Fusion Eng. Des. (ISSN: 0920-3796) 123 (2017) 317–320, http://dx.doi.org/10.1016/j.fusengdes.2017.04.123, URL https://www.sciencedirect.com/science/article/pii/S0920379617305264. Proceedings of the 29th Symposium on Fusion Technology (SOFT-29) Prague, Czech Republic, September 5-9, 2016.

[4] A Lyssoivan, D Douai, R Koch, J Ongena, V Philipps, F C Schüller, D Van Eester, T Wauters, T Blackman, V Bobkov, S Brezinsek, E de la Cal, F Durodié, E Gauthier, T Gerbaud, M Graham, S Jachmich, E Joffrin, A Kreter, V Kyrytsya, E Lerche, P Lomas, F Louche, M Maslov, M-L Mayoral, V Moiseenko, I Monakhov, I Pankratov, M K Paul, R A Pitts, V Plyusnin, G Sergienko, M Shimada, V L Vdovin, JET-EFDA contributors, Simulation of ITER full-field ICWC scenario in JET: RF physics aspects, Plasma Phys. Control. Fusion 54 (7) (2012) 074014, http://dx.doi.org/10.1088/0741-3335/54/7/074014.

[5] D. Douai, D. Kogut, T. Wauters, S. Brezinsek, G.J.M. Hagelaar, S.H. Hong, P.J. Lomas, A. Lyssoivan, I. Nunes, R.A. Pitts, V. Rohde, P.C. de Vries, Wall conditioning for ITER: Current experimental and modeling activities, J. Nucl. Mater. (ISSN: 0022-3115) 463 (2015) 150–156, http://dx.doi.org/10.1016/j.jnucmat.2014.12.034, URL https://www.sciencedirect.com/science/article/pii/S0022311514009763. PLASMA-SURFACE INTERACTIONS 21.

[6] C.A. Balanis, Antenna Theory: Analysis and Design, Wiley, ISBN: 9780471592686, 1996, URL https://books.google.be/books?id=RgmcQgAACAAJ.

[7] P. Dumortier, A.M. Messiaen, ICRH antenna design and matching, Fusion Sci. Technol. 57 (2T) (2010) 230–238, http://dx.doi.org/10.13182/FST10-A9414, arXiv:https://doi.org/10.13182/FST10-A9414.

[8] F. Durodié, M. Vervier, Design of an Automatic Matching Device for Textor's ICRH System, Elsevier, 1991, pp. 1186–1190.

[9] M. Evrard, F. Durodié, P.U. Lamalle, RF circuit simulation of the JET ITER-like ICRH antenna, AIP Conf. Proc. (ISSN: 0094-243X) 787 (1) (2005) 186–189, http://dx.doi.org/10.1063/1.2098220, arXiv:https://pubs.aip.org/aip/acp/article-pdf/787/1/186/11992069/186_1_online.pdf.

[10] Frederic Durodie, Arthur Adriaens, LPP-ERM-KMS/pyRFtk: the python radiofrequency toolkit, initial release, 2023, http://dx.doi.org/10.5281/ZENODO.10391750, URL https://github.com/LPP-ERM-KMS/pyRFtk.

[11] Ansys hfss, 2023, URL https://www.ansys.com/.

[12] V. Maquet, R. Ragona, D. Van Eester, J. Hillairet, F. Durodie, ANSYS HFSS as a new numerical tool to study wave propagation inside anisotropic magnetized plasmas in the ion cylotron range of frequencies, 2023, arXiv:2309.14015.

[13] T.H. Stix, Waves in Plasmas, American Inst. of Physics, ISBN: 9780883188590, 1992, URL https://books.google.be/books?id=OsOWJ8iHpmMC.